Fibers and Polymers 2014, Vol.15, No.12, 2564-2571
DOI 10.1007/s12221-014-2564-y

ISSN 1229-9197 (print version)
ISSN 1875-0052 (electronic version)

Polyamide-Grafted-Multi-walled Carbon Nanotube Electrospun Nanofibers/Epoxy Composites

Ayesha Kausar*

Nanosciences and Catalysis Division, National Centre for Physics, Quaid-i-Azam University Campus, Islamabad 44000, Pakistan

(Received August 23, 2013; Revised July 2, 2014; Accepted July 14, 2014)

Abstract: Multi-walled carbon nanotubes were grafted by polyamide *via* Friedel-Crafts acylation and *in-situ* polymerization routes using γ-Phenyl-ε-caprolactone to obtain MWCNT-PA. Poly(azo-naphthyl-imide) (PI) was also prepared in this work. Afterward, electrospun nanofibers were prepared using grafted nanocarbon fibers in two different polymers; polyimide (PI) and PI/polyaniline (PANI). The obtained nanofibers were used to reinforce an epoxy resin. Scanning and transmission electron microscopy revealed fibrous nature of these composites. The tensile modulus of epoxy composites reinforced by electrospun PI/PANI nanofibers (25.3 GPa) was considerably higher than PI nanofibers (19.8 GPa). In addition, thermal stability of PI/PANI nanofiber composites was superior as having 10 % gravimetric loss at 623-671 °C and glass transition temperature of 289-297 °C relative to MWCNT-PA/PI nanofiber-based system. The addition of 1 to 3 wt% MWCNT-PA/PI/PANI filler content enhanced the electrical conductivity of DGEBA/MWCNT-PA/PI/PANI from 3.33 to 5.99 S cm^{-1}.

Keywords: Polyamide-grafted-carbon nanotube, DGEBA, Friedel-crafts acylation, Electrospun, Thermal stability

Introduction

Epoxy resins have been progressively employed in structural applications varying from high performance aerospace composites to microelectronics industry owing to their high thermal resistance, tensile strength, modulus, and chemical resistance [1-3]. The development of nanoparticle reinforced polymer composites has been one of the most promising approaches in the field of engineering applications [4-7]. The distinctive properties of nanoparticles (carbon nanofiber, carbon nanotube, and carbon black) in combination with conventional reinforcements (polymer fiber such as aramid-fibres), has led to a concentrated research in the field of nanocomposites. Due to the unique properties of carbon nanotube, researchers have focused on utilizing these remarkable characteristics for engineering applications such as polymeric composites, hydrogen storage, actuators, chemical sensors, and nanoelectronic devices [8-10]. Inimitable electronic and mechanical properties of carbon nanotubes (CNT) render polymer/CNT composites commercially important materials [11]. However, the functionalization of nanotube surface has been a significant requisite to enhance its adhesion to the polymer matrix [12,13]. Moreover, exploration of the properties of composites as a function of filler content as well as extent of agglomeration reveals important aspect of these materials [14-17]. On the other hand, contracting the diameters of polymer fiber from 10-100 mm to submicrons or nanometers results in larger surface area to volume ratio, better surface functionalities, and superior mechanical performance compare to other known material. These outstanding properties make the polymer nanofibers to be optimal candidates for many important applications. In current years, a number of processing techniques such as drawing, phase separation, self-assembly, and electrospinning have been used to prepare polymer nanofibers [18-20]. In the electrospinning, a high electric field is generated in polymer solution and metallic collector. The droplets of the polymer solution are converted into cones using electric field and a jet of ultrafine fibers is produced [21]. The advantage of electrospinning is that the polymers can be electrospun in both solution and in a melt state. The electrical, mechanical, and physical properties of polymeric materials can be improved by the inclusion of single walled (SW) or multi-walled (MW) Carbon nanotubes (CNT). However, the dispersion and alignment of filler has problems as they may form bundles and ropes due to Vander Waal's forces. Several approaches have been used in order to obtain a good dispersion and alignment of nanotubes such as chemical functionalization, wrapping, and the synthesis of aligned nanotubes by the deposition of nanotubes onto chemically modified substrate [22-24].

In the present study, the MWCNT was functionalized by Friedel-Crafts acylation reaction, in which 2-(3-amino-propylamino)-nicotinic acid was introduced on the surface of MWCNT using P_2O_5 as drying reagents [25]. Afterward, the polyamide-grafted-nanotubes were electrospun using PI and PI/PANI polymers. The electrospun nanofibers were used to reinforce the epoxy matrix. To investigate the effect of nanofibers, the morphology of nanofibers and nanocomposites were studied using scanning electron microscopy (SEM) and transmission electron microscopy (TEM). Moreover, the electrical conductivity, thermal, and mechanical studies were also carried out on the composites produced. Poly(azo-naphthyl-imide) having naphthalene and heterocyclic imide units was opted to increase the thermal and mechanical

*Corresponding author: asheesgreat@yahoo.com

properties of the composites. Here, the preparation of epoxy systems cured with PI instead of traditional amino-group-containing hardening agents has been focused. During the curing of DGEBA, there was ring opening of epoxide group and then reaction with amide group of polyamic acid formed. Moreover, azo-based polymer was chosen for enhancing the electrical conductivity of the material. Another conducting polymer i.e. polyaniline was also included in the composite structure to further improve the electrical conductivity of the composite. The probable interaction between polyaniline and epoxy was the π-π interaction between the polymers. The chemical interaction also exists between secondary amine functionality of modified nanotubes and epoxide group of DGEBA.

Experimental

Materials

Multi-walled carbon nanotubes were prepared according to the previously reported procedure [26]. Bisphenol A diglycidyl ether (DGEBA), pyromellitic dianhydride (PMDA) (97 %), 1,5-diaminonaphthalene (97 %) 1,4-phenylenediamine (PDA) (97 %), γ-phenyl-ε-caprolactone (99 %), 2-(3-amino-propylamino)-nicotinic acid (99 %), stannous octoate (95 %), polyphosphoric acid (≥83 % phosphate), phosphoric pentaoxide (P_2O_5, 99 %) and N,N-dimethylacetamide (DMAc) (99 %) were procured from Aldrich (St. Louis, Missouri, USA). Ammonium thiocyanate (98 %) was provided by Fluka (Biocen GmbH, Duesseldorf, Germany).

Equipments

Infrared (IR) spectra were recorded using Fourier transform infrared (FTIR) Spectrometer, Model No. FTSW 300 MX, manufactured by BIO-RAD, California, USA (4 cm^{-1} resolution). Nuclear magnetic resonance (NMR) spectra were scanned at room temperature using BRUKER (Tokyo, Japan) Spectrometer (300.13 MHz for ^1H NMR) in deuterated dimethyl sulfoxide (DMSO-d_6). The number and weight average molecular weight of polymers were calculated through gel-permeation chromatography (GPC) and refractive index (RI) detector. Field Emission Scanning Electron Microscopy (FE-SEM) of frozen fractured samples was performed using JSM5910, JEOL Japan. Transmittance electron microscope (TEM) was performed with a LEO 912 Omega instrument at 120 kV. The ultra thin sections were prepared at -60 °C with an Ultracut E ultramicrotome using diamond knife. Thermal stability was verified by METTLER TOLEDO TGA/SDTA 851 (California, USA) thermo gravimetric analyzer using 1-5 mg of the sample in Al_2O_3 crucible at a heating rate of 10 °C/min. The dynamic mechanical thermal analysis (DMTA) was performed on hybrid materials in the temperature range of 0-300 °C with DMTA Q800 (frequency of 5 Hz, heated at 10 °C/min). Stress-strain response of the samples was obtained on Universal Testing Machine INSTRON 4206 (Norwood, United States) according to the ASTM 638 method. A crosshead speed of 100 mm/min was used during the test. Electrical conductivity of thin films was measured using a Keithley 614 electrometer and the four-probe method.

Diazotization

1,5-Diaminonaphthalene (0.04 mol) was added to 10 m*l* of hydrochloric acid (ACS reagent, 37 %) and 50 m*l* water to dissolve it. The mixture was placed in ice-bath to cool to -10 °C. A solution of sodium nitrite (2 M) was then added with continuous stirring. After the complete addition, the mixture was allowed to stir for 1 h at -10 °C to avoid the decomposition of diazonium salt. The excess of nitrite was removed by the addition of urea (2 g) with stirring of 0.5 h forming diazonium salt solution [27].

Synthesis of Poly(azo-naphthyl-imide) (PI)

To synthesis the polymer, 250 m*l* round bottom flask was charged with 0.01 mol 1,4-phenylene bis(thiourea) [28] and 50 m*l* DMAc. The mixture was stirred at 0 °C for 0.5 h. Afterwards, 0.01 mol pyromellitic dianhydride and diazonium salt solution was added and the mixture was again stirred at 0 °C for 1 h. Later the mixture was allowed to stir at room temperature for 24 h. The poly(amic acid) was precipitated by pouring the flask content into 200 m*l* water and methanol mixture. Then it was filtered, washed with hot water, and dried overnight under vacuum at 70 °C. In a 250 m*l* two-necked round bottom flask, 1.0 g of poly(amic acid) was dissolved in 5 m*l* dry DMAc, 5 m*l* acetic anhydride and 2.5 m*l* pyridine were then added to the above mixture and

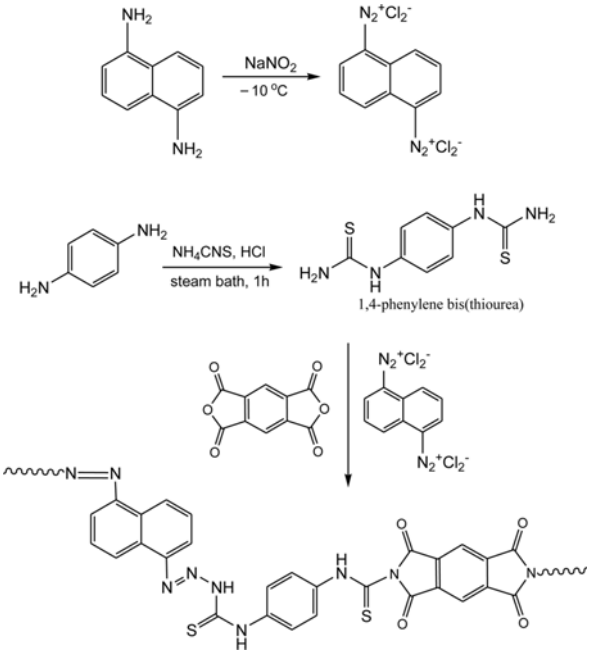

Scheme 1. Preparation of poly(azo-naphthyl-imide).

Table 1. Sample composition and abbreviations

Composition	Abbreviation	Short name
Poly(azo-naphthyl-imide)	PI	Polyimide
Multi-walled carbon nanotubes/polyamide/poly(azo-naphthyl-imide) nanofiber	MWCNT-PA/PI	
Multi-walled carbon nanotubes/polyamide/poly(azo-naphthyl-imide)/ polyaniline nanofiber	MWCNT-PA/PI/PANI	
Epoxy/multi-walled carbon nanotubes/polyamide/poly(azo-naphthyl-imide)/ polyaniline nanofiber (1 wt%)	DGEBA/MWCNT-PA/PI/PANI 1	
Epoxy/multi-walled carbon nanotubes/polyamide/poly(azo-naphthyl-imide)/ polyaniline nanofiber (2 wt%)	DGEBA/MWCNT-PA/PI/PANI 2	Epoxy/polyaniline nanofibers
Epoxy/multi-walled carbon nanotubes/polyamide/poly(azo-naphthyl-imide)/ polyaniline nanofiber (3 wt%)	DGEBA/MWCNT-PA/PI/PANI 3	
Epoxy/multi-walled carbon nanotubes/polyamide/poly(azo-naphthyl-imide) nanofiber (1 wt%)	DGEBA/MWCNT-PA/PI 1	
Epoxy/multi-walled carbon nanotubes/polyamide/poly(azo-naphthyl-imide) nanofiber (2 wt%)	DGEBA/MWCNT-PA/PI 2	Epoxy/polyamide-imide nanofibers
Epoxy/multi-walled carbon nanotubes/polyamide/poly(azo-naphthyl-imide) nanofiber (3 wt%)	DGEBA/MWCNT-PA/PI 3	

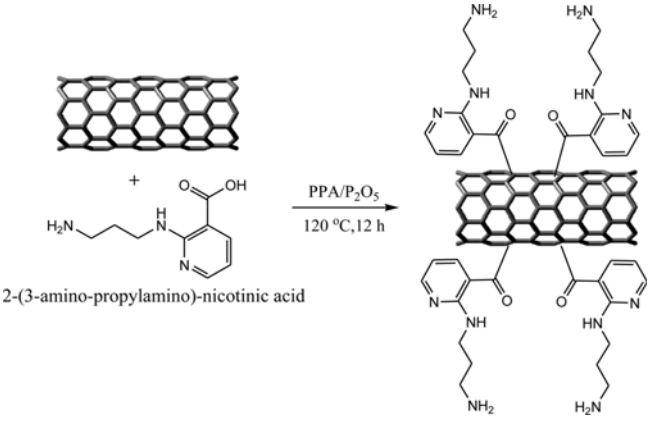

Scheme 2. Friedel-Crafts acylation of side walls of MWCNT.

heated to 80 °C for 6 h. The mixture was cooled and poured into water. Finally, it was filtered, washed with hot water and methanol, and dried under vacuum at 90 °C (Scheme 1). The molecular weight (M_w) of synthesized poly(azo-naphthyl-imide) was obtained to be as high as 31×10^3 gmol^{-1}. The structure of the polymer was characterized and presented in Table 1.

Functionalization of MWCNT *via* Friedel-Crafts Acylation

Scheme 2 shows the side-wall functionalization of MWCNT. In Friedel-Crafts acylation, 2-(3-amino-propylamino)-nicotinic acid, MWCNT, and polyphosphoric acid were mixed and heated at 120 °C for 3 h. Then, phosphoric penta oxide (P_2O_5) was added to the mixture and heated for further 12 h. The reaction mixture was cooled, diluted with distilled water, and filtered. The functionalized MWCNT were dried at 100 °C for 48 h [29].

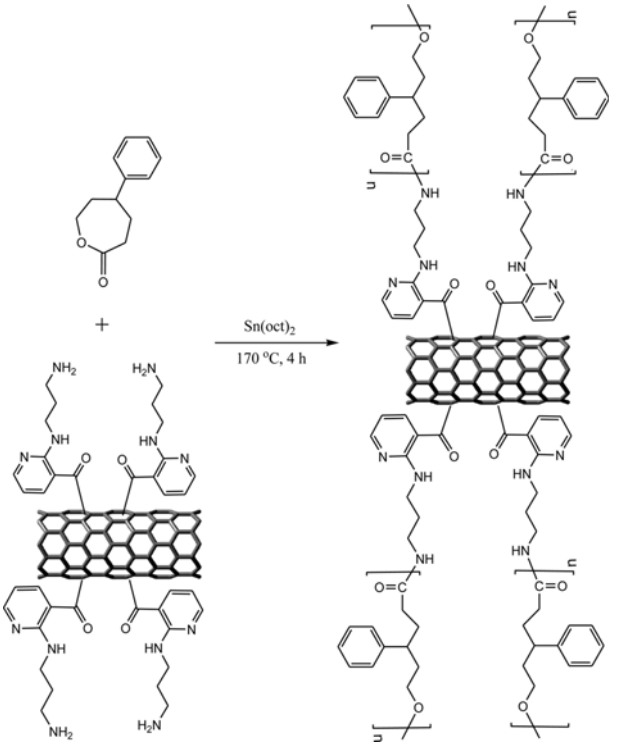

Scheme 3. Formation of MWCNT-PA *via in-situ* polymerization.

Formation of MWCNT-PA *via In-situ* Polymerization

Functionalized MWCNT (0.1 g) and γ-phenyl-ε-caprolactone (20 m*l*) were sonicated at room temperature for 3 h to obtain homogeneous dispersion of nanotube. Stannous octoate $Sn(Oct)_2$ (0.03 m*l*) was added to the above suspension [30]. The reaction flask was then heated to 170 °C for 4 h with

mechanical stirring under nitrogen atmosphere (Scheme 3).

Polymer Solution Preparation for Electrospinning

For the preparation of MWCNT-PA/PI solution for electrospinning, a solution contained 5 wt% MWCNT-PA and 25 wt% PI was prepared in DMAc. For MWCNT-PA/PI/PANI, 25 wt% PI solution was diluted with 5 wt% MWCNT-PA and 5 wt% PANI/DMAc solution. Prior to solution mixing, the MWCNT-PA/DMAc solution was sonicated for 5 h to disperse the carbon nanotube homogeneously.

Preparation of Nanofiber *via* Electrospinning

Electrospinning was carried out using a syringe with a spinneret (diameter 0.5 mm) and 25 kV applied voltage at 30 °C. The feeding rate was 0.25 m*l*/h and the spinneret-collector distance was set to be 10 cm. Two types of nanofibers MWCNT-PA/PI and MWCNT-PA/PI/PANI were collected using a rotating disk collector (diameter 0.30 m; width 10 mm). During electrospinning, the linear speed of rotating collector was about 10 ms^{-1}. All the electrospun nanofibers were dried at 100 °C for 4 h to remove the residual solvent.

Preparation of Nanofiber Reinforced Films

An amount of 1, 2, and 3 wt% of as-prepared electrospun (MWCNT-PA/PI and MWCNT-PA/PI/PANI) nanofibers were immersed in 2 g DGEBA for 1 h and heated to 100 °C to obtain the nanofiber reinforced nanocomposite films with different nanofiber contents. Table 1 shows the chemical structural characterization of DGEBA/MWCNT-PA/PI and DGEBA/MWCNT-PA/PI/PANI nanofiber reinforced nanocomposite. Sample composition, designation and short names used are mentioned in Table 1.

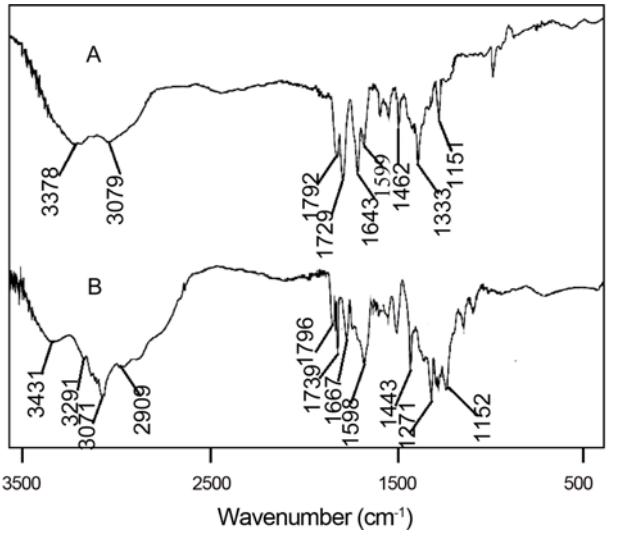

Figure 1. FTIR spectra of (A) MWCNT-PA/PI/PANI nanofiber and (B) DGEBA/MWCNT-PA/PI/PANI 1.

Results and Discussion

Fabrication of Nanofibers and Nanocomposites

In this attempt, the properties of epoxy based nanocomposites reinforced by polyamide-grafted-nanotube nanofibers electrospun in two different polymers, poly(azo-pyridine-benzophenone-imide) and polyaniline, were reported and compared. The chemical and bond structure of electrospun nanofibers and nanocomposites were investigated using FTIR. Figure 1 and Table 2 represent the spectral data for

Table 2. Structural analysis data of neat PI, nanofiber, and nanocomposite

Compound	FTIR		NMR
	Type of vibration	Frequency (cm^{-1})	^{1}H NMR (δ ppm)
PI	N-H stretch	3332	9.21 (s) Sec. Amine
	Aromatic C-H stretch	3013	8.89 (s) Anhydride ring protons
			7.23, 7.74 (d) 7.12 (t) naphthalene aromatic protons
	Imide C=O (Symmetric)	1796	6.23-6.48 (d) Phenylene protons
	Imide C=O (Asymmetric)	1728	
	N-H bend	1599	
	-N=N-	1413	
	C-O	1270	
	C=S	1126	
MWCNT-PA/PI/PANI nanofiber	N-H stretch	3378	
	Aromatic C-H stretch	3079	
	Imide C=O (Symmetric)	1792	
	Imide C=O (Asymmetric)	1729	
	Amide C=O	1643	
	N-H bend	1599	
	-N=N-	1462	
	C=S	1151	
DGEBA/MWCNT-PA/PI/PANI 1	O-H stretch	3431	
	N-H stretch	3291	
	Aromatic C-H stretch	3071	
	Aliphatic C-H stretch	2909	
	Imide C=O(Symmetric)	1796	
	Imide C=O (Asymmetric)	1739	
	Amide C=O	1667	
	N-H bend	1598	
	-N=N-	1443	
	C-O	1243	
	C=S	1152	

MWCNT-PA/PI/PANI nanofiber and epoxy nanocomposite contained 1 wt% nanofiber. The results were in agreement with the proposed structures. Hydroxyl group of DGEBA showed broad stretching vibration at 3431 cm^{-1} in the nanocomposite (Figure 1(B)). However, this peak was absent in the case of MWCNT-PA/PI/PANI. Furthermore, due to ring opening of epoxide during the reaction with amine, DGEBA/MWCNT-PA/PI/PANI depicted an aliphatic stretching vibration at 2909 cm^{-1}. This peak was also disappeared in the case of relevant nanofiber (Figure 1(A)). The spectrum of nanocomposite also showed secondary amine stretching and bending vibrations at 3291 and 1598 cm^{-1}. Azo (-N=N-) and thiourea (C=S) groups were appeared at 1443 and 1152 cm^{-1}, respectively. In DGEBA/MWCNT-PA/PI/PANI 1, C-O characteristic stretch was also observed around 1243 cm^{-1}. Alternatively, in nanofiber, secondary amine stretching and bending vibrations were at 3378 and 1599 cm^{-1} and azo (-N=N-) and thiourea (C=S) groups were appeared at 1462 and 1151 cm^{-1}, respectively. In addition, peaks at 1792, 1729, and 1643 cm^{-1} are related to imide and amide carbonyl. Nanocomposite showed these vibrations at 1796, 1739, and 1667 cm^{-1} confirming the structure of MWCNT-polyamide/polyimide. The appearance of the amide group indicated that the polyamide chains were chemically bonded to the side wall of MWCNT.

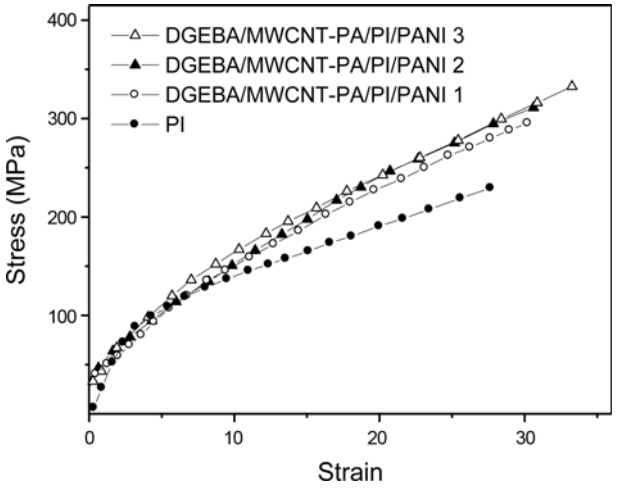

Figure 2. Stress-strain curves of neat PI and DGEBA/MWCNT-PA/PI/PANI nanocomposites.

Tensile Strength of DGEBA/MWCNT-PA/PI and DGEBA/MWCNT-PA/PI/PANI

The tensile properties of DGEBA/MWCNT-PA/PI and DGEBA/MWCNT-PA/PI/PANI composites contained 1 to 3 wt% nanofibers are shown in Figure 2 and Table 3. The tensile strength of nanocomposites was gradually enhanced by increasing filler contents. The maximum stress value was observed for DGEBA/MWCNT-PA/PI/PANI (3 wt%) as 332.6 MPa. Also, MWCNT-PA/PI/PANI (1 wt%) had elongation at break value of 30.2 % that increased to 33.5 % by adding 3 wt% nanofibers. The initial modulus for DGEBA/MWCNT-PA/PI/PANI (1 wt%) was enhanced from 21.1 GPa to 25.3 GPa for Epoxy/polyaniline nanofibers (3 wt%). Toughness, calculated by integrating the area under stress-strain curves, of Epoxy/polyaniline nanofibers (1 wt%) showed value of 5576 MPa that increased by adding reinforcement and was obtained to be maximum (6916 MPa) for 3 wt% nanofiber content. On the other hand, Epoxy composites reinforced by MWCNT-PA/PI showed comparatively lower value in tensile properties. Tensile strength and elongation at break were ranged between 244.4 to 249.9 MPa and 28.5 to 29.3 %, respectively. Tensile modulus was around 15.9-19.8 GPa which was lower than Epoxy/polyaniline nanofibers-based material. Experiential increase in tensile strength of Epoxy/polyaniline nanofibers nanocomposites may be attributed to the nanofiber structure in which MWCNT-PA composed the core coated with polyimide and PANI. Moreover, the alignment of nanofibers in epoxy, due to doubly layered polymers, induced uniform wrapping of matrix on nanofiber surface. Finally, the stress transfer or strength of DGEBA/MWCNT-PA/PI/PANI nanocomposites was effectively enhanced by the chemical interaction between epoxide group of the matrix and amine group of nanofibers [31].

Table 3. Mechanical properties of pristine PI, DGEBA/MWCNT-PA/PI/PANI and DGEBA/MWCNT-PA/PI films

Composition	Tensile stress (MPa) ±0.1	Elongation at break (%) ±0.03	Tensile modulus (GPa) ±0.1	Toughness (MPa)[1] ±0.2
PI	212.2	27.8	15.2	4222
DGEBA/MWCNT-PA/PI/PANI 1[2]	295.4	30.2	21.1	5576
DGEBA/MWCNT-PA/PI/PANI 2	326.4	31.6	23.2	7143
DGEBA/MWCNT-PA/PI/PANI 3	332.6	33.5	25.3	6916
DGEBA/MWCNT-PA/PI 1	244.4	28.2	15.9	4321
DGEBA/MWCNT-PA/PI 2	246.1	28.5	17.7	4434
DGEBA/MWCNT-PA/PI 3	249.9	29.3	19.8	5332

[1]Toughness was determined by integrating the area under the stress-strain curve and [2]the number in the sample designation refers to wt% of nano-fibers in the sample.

Morphology

Morphological study of the fracture surfaces of MWCNT-PA/PI nanofibers, MWCNT-PA/PI/PANI nanofibers and DGEBA/MWCNT-PA/PI/PANI 1-3 nanocomposites were analyzed by SEM image presented in Figure 3. MWCNT-PA/PI/PANI fibers (Figure 3(B)) were found to orderly aligned and homogeneously electrospun relative to MWCNT-PA/PI (Figure 3(A)). An important factor was the effective interfacial interaction between the polymers and MWCNT in these electrospun nanofibers. Moreover, the processing conditions of manufacturing procedure were important to facilitate the effective interfacial interaction between the polyamide/polyimide and MWCNT in these nanofibers. Accordingly, the electrospun MWCNT-PA/PI/PANI nanofibers were relatively smooth, uniformly aligned and almost free of defects. Alternatively, DGEBA reinforced with the electrospun MWCNT-PA/PI/PANI nanofibers displayed different morphology (Figure 3(C)-(E)). Addition of 1 wt% MWCNT-PA/PI/PANI nanofibers had random orientation in the matrix due to poor dispersion (Figure 3(C)). Epoxy/polyaniline nanofibers-based material having 2 wt% filler (Figure 3(D)) showed relatively good alignment of filler in the matrix and the nanofibers were unvaryingly coated with DGEBA. The incorporation of greater MWCNT-PA/PI/PANI (Figure 3(E)) content resulted in the further widening of the polymer coated nanofiber diameter and their haphazard distribution in the matrix. Hence, the optimum matrix to fibers ratio is essential for good dispersion of nanofiber in epoxy resulting in fine morphology. TEM micrographs of the electrospun MWCNT-PA/PI/PANI nanofiber and DGEBA/MWCNT-PA/PI/PANI 1 nanocomposite are given in Figure 4(A) & (B). The study confirmed the morphological observation by SEM. MWCNT-PA/PI/PANI nanofiber had smaller diameter according to Figure 4(A). Whilst, Figure 4(B) portrayed the coating of DGEBA around MWCNT-PA/PI/PANI so evading the aggregation of individual nanofiber. Both the nanofiber and nanocomposite had a typical core-shell structure. In nanofiber, the MWCNT-PA served as the core, which was dispersed into PI and PANI matrices. However, in Epoxy/polyaniline nanofibers-based material with 1 wt% filler, the single tube size is increased due to MWCNT-PA entrapped in epoxy. MWCNT-PA/PI/PANI were not simply mixed up or blended with the DGEBA, but they were rather glued or bound by matrix. Thus, the matrix prevented MWCNT-PA/PI/PANI from agglomeration. Electrospinning of polymer with carbon nanotubes render fine alignment to the nanofibers.

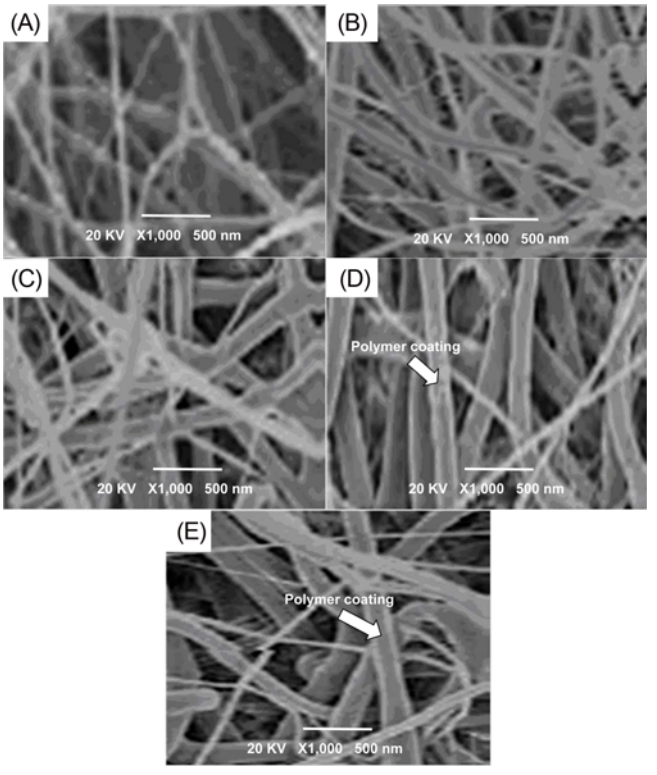

Figure 3. FESEM images of (A) MWCNT-PA/PI nanofibers, (B) MWCNT-PA/PI/PANI nanofibers, (C) DGEBA/MWCNT-PA/PI/PANI 1, (D) DGEBA/MWCNT-PA/PI/PANI 2, and (E) DGEBA/MWCNT-PA/PI 1/PANI 3.

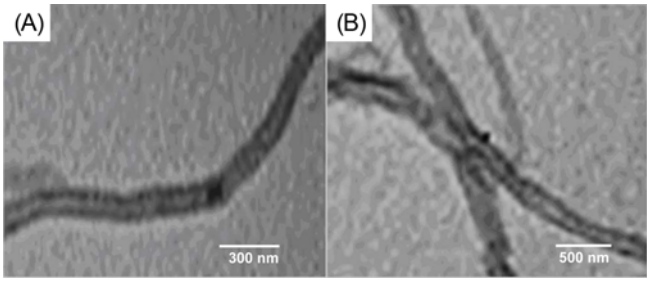

Figure 4. TEM images of (A) MWCNT-PA/PI/PANI nanofibers and (B) DGEBA/MWCNT-PA/PI/PANI 1.

Thermal Properties

Thermal stability of PI, DGEBA/MWCNT-PA/PI/PANI and DGEBA/MWCNT-PA/PI films was examined with TGA. Table 4 shows the initial decomposition temperature (T_0), temperature for 10 % weight loss (T_{10}), and maximum decomposition temperature (T_{max}). According to literature, MWCNT are very stable and no decomposition takes place upto 600 °C as shown in Figure 5. Major step of weight loss for PI occurred above 550 °C. The T_0 occurred at 552 °C, T_{10} around 581 °C, and T_{max} of 615 °C was observed. In DGEBA/MWCNT-PA/PI/PANI 1, 1 wt% addition of MWCNT-PA/PI/PANI nanofibers in matrix resulted in higher thermal properties (T_0=573 °C, T_{10}=623 °C, and T_{max}=678 °C). Epoxy/polyaniline nanofibers with 2 wt% filler in the polymer matrix increased the thermal properties compared to PI and 1 wt% epoxy composite. Consequently, 3 wt% MWCNT-PA/PI/PANI nanofibers further increased the stability. Additionally, the char yield of epoxy/polyaniline nanofibers-

Table 4. Thermal analyses data of pristine PI, DGEBA/MWCNT-PA/PI/PANI, and DGEBA/MWCNT-PA/PI films

Polymer	T_g (°C)	T_0 (°C)	T_{10} (°C)	T_{max} (°C)	Y_c at 800 °C (%)
PI	238	552	581	615	35
DGEBA/MWCNT-PA/PI/PANI 1	289	573	623	678	48
DGEBA/MWCNT-PA/PI/PANI 2	292	594	644	696	61
DGEBA/MWCNT-PA/PI/PANI 3	297	598	671	778	69
DGEBA/MWCNT-PA/PI 1	243	565	588	632	39
DGEBA/MWCNT-PA/PI 2	247	572	599	647	41
DGEBA/MWCNT-PA/PI 3	252	581	601	654	52

T_g: glass transition temperature, T_0: initial decomposition temperature, T_{10}: temperature for 10 % weight loss, T_{max}: maximum decomposition temperature, and Y_c: char yield; weight of polymer remained.

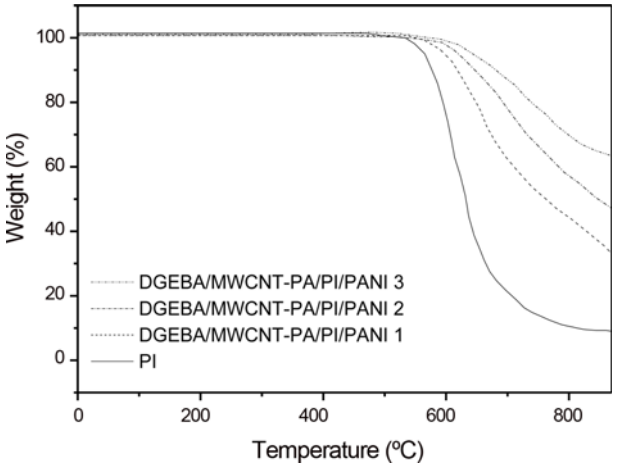

Figure 5. TGA curves of neat PI and DGEBA/MWCNT-PA/PI/PANI films at a heating rate 10 °C/min in N_2.

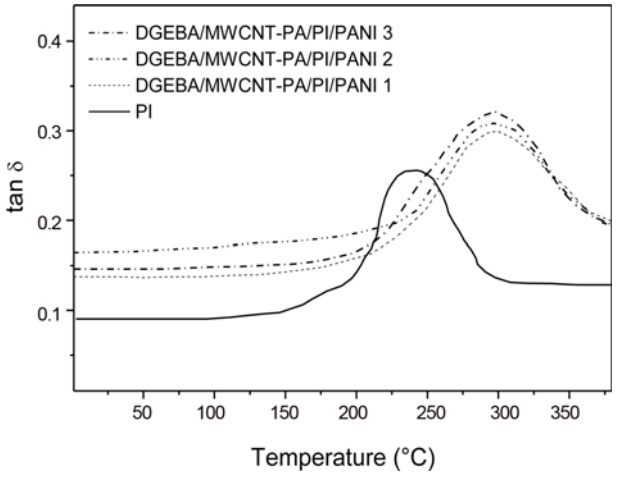

Figure 6. Variation of loss tangent (tanδ) with temperature for pure polymer and DGEBA/MWCNT-PA/PI/PANI films.

based nanohybrids was found in the range 48-69 % at 800 °C. Thermal stability was found to be lower for MWCNT-PA/PI reinforced films (DGEBA/MWCNT-PA/PI 1-3). Correspondingly, the char yield of these nanohybrids was relatively lower. Dynamic mechanical analysis was used to find out the glass transition temperature (T_g) of the nanocomposite films. Figure 6 shows that the loss tangent (tan ε) of DGEBA/MWCNT-PA/PI/PANI 1-3 had T_g of 289-297 °C. Whereas, in the case of epoxy/polyamide-imide nanofibers-based composites T_g was 243-252 °C. Higher T_g for MWCNT-PA/PI/PANI 1-3 was attributed to two types of polymers polyamide (chemically linked) and polyimide (coated) were responsible for the MWCNT/polymer structural stiffness in this nanocomposites. The series without polyaniline possessed lower T_g's due to relatively lower chain packing and stiffness. However, in both series the material containing 3 wt% MWCNT-PA/PI/PANI or MWCNT-PA/PI nanofibers owned higher tan δ and T_g suggestive of increase in chain stiffness with filler loading. Furthermore, the values of both nanocomposite series were notably higher than neat polyimide 238 °C. In summary, the electrospun nanofibers were useful contenders for fabricating high performance epoxy nanocomposites relative to reported ones [32].

Table 5. Conductivity measurement of nanocomposites

Sample	Conductivity (S cm^{-1})
DGEBA/MWCNT-PA/PI/PANI 1	3.33
DGEBA/MWCNT-PA/PI/PANI 2	4.57
DGEBA/MWCNT-PA/PI/PANI 3	5.99
DGEBA/MWCNT-PA/PI 1	2.97
DGEBA/MWCNT-PA/PI 2	3.12
DGEBA/MWCNT-PA/PI 3	3.77

Electrical Conductivity

Table 5 presents the electrical conductivity of DGEBA/MWCNT-PA/PI/PANI 1-3 and DGEBA/MWCNT-PA/PI 1-3 nanocomposites. Nanofibers along with azo-based polyimide and polyaniline were found to improve the conductivity of corresponding nanocomposites. The conductivity of DGEBA/MWCNT-PA/PI/PANI 1 was 3.33 Scm^{-1}, which was increased with the addition of MWCNT-PA/PI/PANI to 5.99 Scm^{-1} (3 wt%). Alternatively, DGEBA/MWCNT-PA/PI 1 had

conductivity of 2.97 Scm^{-1} which was enhanced to 3.77 Scm^{-1} in DGEBA/MWCNT-PA/PI 3. The improvement of conductivity in epoxy/polyaniline nanofibers-based material was credited to the inclusion of conducting polyaniline in nanofibers [33].

Conclusion

Polyamide-grafted-MWCNT was prepared by *in-situ* polymerization. The functional nanotube was then electrospun with poly(azo-naphthyl-imide) and polyaniline to form two types of nanofibers MWCNT-PA/PI and MWCNT-PA/PI/PANI. The MWCNT-PA was embedded within nanofibers and was well oriented along the axes of the nanofibers during electrospinning. Moreover, nanofibers were electrospun from the same MWCNT-PA solutions concentrations. The resulting nanofibers were then used as reinforcing materials in DGEBA matrix. The composites reinforced by MWCNT-PA/PI/PANI had better, mechanical, thermal, and electrical profiles compared to composites reinforced by MWCNT-PA/PI. Inclusion of PANI in nanofibers considerably increased the conductivity of nanocomposites up to 5.99 S cm^{-1}. Epoxy/polyaniline nanofibers-based material revealed higher glass transition temperature in the range of 289-297 °C compared to MWCNT-PA/PI reinforced system with T_g= 243-252 °C. MWCNT-PA/PI/PANI loading also increased the tensile strength of the composites up to 332.6 MPa, while the tensile strength of Epoxy/polyamide-imide system was enhanced up to 249.9 MPa. The fallouts proved that MWCNT-PA/PI/PANI nanofibers were better reinforcing material for epoxy. Utilizing these remarkable characteristics of new epoxy/electrospun nanofibers, these high performance materials may find wide range of scope in several engineering applications such as aerospace structural parts.

References

1. Y. J. Kim, T. S. Shin, H. D. Choi, J. H. Kwon, Y. Chung, and H. G. Yoon, *Carbon,* **43**, 23 (2005).
2. F. H. Gojny, M. H. G. Wichmann, B. Fiedler, W. Bauhofer, and K. Schulte, *Compos. Pt. A-Appl. Sci. Manuf.,* **36**, 1525 (2005).
3. Y. Liao, O. M. Tondin, Z. Liang, C. Zhang, and B. Wang, *Mater. Sci. Eng. A.,* **385**, 175 (2004).
4. S. Cui, R. Canet, A. Derre, M. Couzi, and P. Delhaes, *Carbon,* **41**, 797 (2003).
5. K. T. Lau, S. Q. Shi, and H. M. Cheng, *Compos. Sci. Technol.,* **63**, 1161 (2003).
6. J. K. W. Sandler, J. E. Kirk, I. A. Kinloch, M. S. P. Shaffer, and A. H. Windle, *Polymer,* **44**, 5893 (2003).
7. X. Li, H. Gao, W. A. Scrivens, D. Fei, X. Xu, and M. A. Sutton, *Nanotechnology,* **15**, 1416 (2004).
8. F. H. Gojny, J. Nastalczyk, Z. Roslaniec, and K. Schulte, *Chem. Phys. Lett.,* **370**, 820 (2003).
9. C. A. Martın, J. K. W. Sandler, M. S. P. Shaffer, M. K. Schwarz, W. Bauhofer, K. Schulte, and A. H. Windle, *Compos. Sci. Technol.,* **64**, 2309 (2004).
10. A. Allaoui, A. S. Bai, H. M. Cheng, and J. B. Bai, *Compos. Sci. Technol.,* **62**, 1993 (2002).
11. Y. Breton, G. Desarmot, J. P. Salvetat, S. Delpeux, C. Sinturel, F. Beguin, and S. Bonnamy, *Carbon,* **42**, 1027 (2004).
12. H. Miyagawa and L. T. Drzal, *Polymer,* **45**, 5163 (2004).
13. S. J. Park, H. J. Jeong, and C. Nah, *Mater. Sci. Eng. A*, **385**, 13 (2004).
14. A. Celzard, E. McRae, C. Deleuze, M. Dufort, G. Furdin, and J. F. Mareche, *Phys. Rev. B,* **53**, 6209 (1996).
15. P. Potschke, A. R. Bhattacharyya, and A. Janke, *Eur. Polym. J.,* **40**, 137 (2004).
16. P. Potschke, T. D. Fornes, and D. R. Paul, *Polymer,* **43**, 3247 (2002).
17. Y. S. Song and J. R. Youn, *Carbon,* **43**, 1378 (2005).
18. T. Ondarcuhu and C. Joachim, *Europhys. Lett.,* **42**, 215 (1998).
19. G. J. Liu, J. F. Ding, L. J. Qiao, A. Guo, B. P. Dymov, J. T. Gleeson, T. Hashimoto, and K. Saijo, *Chem-A Eur. J.,* **5**, 2740 (1999).
20. G. M. Whitesides and B. Grzybowski, *Science*, **295**, 2418 (2002).
21. B. Vigolo, A. Pénicaud, C. Coulon, C. Sauder, R. Pailler, C. Journet, P. Bernier, and P. Poulin, *Science,* **290**, 1331 (2000).
22. M. Holzinger, O. Vostrowsky, A. Hirsch, F. Hennrich, M. Kappes, R. Weiss, and F. Jellen, *Angew. Chem. Int. Ed.,* **40**, 4002 (2001).
23. A. Hirsch, *Angew. Chem. Int. Ed.,* **41**, 1853 (2002).
24. R. R. Schlittler, J. W. Seo, J. K. Gimzewski, C. Durkan, M. S. M. Saifullah, and M. E. Welland, *Science,* **292**, 1136 (2001).
25. J.-B. Baek, S.-Y. Park, G. E. Price, C. B. Lyons, and L. S. Tan, *Polymer,* **46**, 1543 (2005).
26. S. T. Hussain, *U.S. Patent,* 2009208403 (2009).
27. H. Diener, B. Gulec, P. Skrabal, and H. Zollinger, *Helv. Chim. Acta,* **72**, 800 (2004).
28. S. F. Fennessey and R. J. Farris, *Polymer,* **45**, 4217 (2004).
29. J.-B. Baek and L. S. Tan, *Polymer,* **44**, 4135 (2003).
30. K. Saeed, S.-Y. Park, S. Haider, and J.-B. Baek, *Nanoscale Res. Lett.,* **4**, 39 (2008).
31. G. Park, Y. Jung, G.-W. Lee, J. P. Hinestroza, and Y. Jeong, *Fiber. Polym.,* **13**, 874 (2012).
32. B. G. Demczyk, Y. M. Wang, J. Cumings, M. Hetman, W. Han, A. Zettl, and R. O. Ritchie, *Mater. Sci. Eng. A.,* **334**, 173 (2002).
33. A. Kausar and S. T. Hussain, *J. Plast. Film. Sheet*., **29**, 365 (2013).